Carbon nanotube modified air-cathodes for electricity production in microbial fuel cells

Heming Wang [a], Zhuangchun Wu [b], Atousa Plaseied [c], Peter Jenkins [c], Lin Simpson [b], Chaiwat Engtrakul [b], Zhiyong Ren [a,*]

[a] Department of Civil Engineering, University of Colorado Denver, Denver, CO 80217, United States
[b] National Renewable Energy Laboratory, 1617 Cole Blvd., Golden, CO 80401, United States
[c] Department of Mechanical Engineering, University of Colorado Denver, Denver, CO 80217, United States

ABSTRACT

The use of air-cathodes in microbial fuel cells (MFCs) has been considered sustainable for large scale applications, but the performance of most current designs is limited by the low efficiency of the three-phase oxygen reduction on the cathode surface. In this study we developed carbon nanotube (CNT) modified air-cathodes to create a 3-D electrode network for increasing surface area, supporting more efficient catalytic reaction, and reducing the kinetic resistance. Compared with traditional carbon cloth cathodes, all nanotube modified cathodes showed higher performance in electrochemical response and power generation in MFCs. Reactors using carbon nanotube mat cathodes showed the maximum power density of $329\,mW\,m^{-2}$; more than twice that of the peak power obtained with carbon cloth cathodes ($151\,mW\,m^{-2}$). The addition of Pt catalysts significantly increased the current densities of all cathodes, with the maximum power density obtained using the Pt/carbon nanotube mat cathode at $1118\,mW\,m^{-2}$. The stable maximum power density obtained from other nanotube coated cathodes varied from $174\,mW\,m^{-2}$ to $522\,mW\,m^{-2}$. Scanning electron micrographs showed the presence of conductive carbon nanotube networks on the CNT modified cathodes that provide more efficient oxygen reduction.

© 2011 Elsevier B.V. All rights reserved.

1. Introduction

Microbial fuel cells (MFCs) are renewable energy systems that employ bacteria to convert chemical energy stored in biodegradable materials to electrical energy. The MFC technology carries great potential as it concurrently removes pollutants from the environment and produces energy. An MFC reactor generally consists of an anode, a cathode, and sometimes a separator between the two electrodes [1]. In order to provide good access for bacteria and improve power generation, the electrodes in MFCs need to have high surface area, high conductivity, and be resistant to physical and chemical corrosion. Many anode materials have been tested, including woven graphite mat [2], carbon paper [3], carbon cloth [4], and activated carbon [5]. A recent development of graphite brush anodes provides a solution for scaling up because it has very high specific surface area ($7170–18,200\,m^2\,m^{-3}$) and an open structure to prevent fouling problems [6]. Moreover, this makes the anode no longer the main limitation on power production, but

instead brings up the challenge of effective cathode development [7,8].

Even though ferricyanide or permanganate can provide a higher cathode open circuit potential, oxygen is considered as the electron acceptor for eventual MFC applications due to its availability and high redox potential ($E^0 = 1.23\,V$) [8,9]. However, the tri-phase reaction among oxygen gas, solid catalyst, and liquid electrolyte does not make satisfactory reaction kinetics. Moreover, the specific surface area ($\sim100\,m^2\,m^{-3}$) of current popular air-cathode designs are orders of magnitude lower compared with the brush anode, making the cathode the primary limiting factor for improved power production in MFCs. Previous results showed that MFC power output improved along with the increase of cathode specific surface area. For example, Deng et al., found the power density increased from $67\,mW\,m^{-2}$ to $315\,mW\,m^{-2}$ by replacing carbon paper cathodes with high specific surface area activated carbon felt cathodes [10]. Cheng and Logan recently demonstrated that the volumetric power density has a linear relationship with the cathode specific surface area [11].

Carbon nanotubes (CNTs) have exhibited great potential as electrode materials in fuel cell applications due to their high surface-to-volume ratio and unique electrical and mechanical properties. Several studies investigated the performance of CNT-

* Corresponding author. Tel.: +1 303 556 5287; fax: +1 303 556 2368.
E-mail addresses: zhiyong.ren@ucdenver.edu, zzr101psu@gmail.com (Z. Ren).

modified anodes in MFCs and found that the anode biofilm activity was not affected by the carbon nanotubes but the power density was improved [12–14]. Though the CNT-modified anodes do not provide direct large enough macro-scale porosity for more microbial colonization, the highly conductive nanotube network serves as nanowires to facilitate the electron transfer between the microbes to the electrodes. The reported power densities obtained from CNT-modified anodes varied from $22\,mW\,m^{-2}$ (multi-walled CNT) [15] to $1098\,mW\,m^{-2}$ (3-D CNT-textile) [13]. However, to date little effort has been reported on CNT-modified cathodes, even though the benefits can be more significant because the CNT-modified cathodes provide higher conductivity for improved electron transfer efficiency and allow more nano-sized catalyst particles to be deposited in a 3D texture to facilitate the tri-phase reaction kinetics. Therefore, in this study we used carbon nanotubes to modify the air-cathode using several different methods and characterized the MFC performance under each condition.

2. Materials and methods

2.1. Cathode construction

Different coating methods were used to modify MFC air-cathodes using carbon nanotubes. In addition, carbon nanotube mat and carbon cloth modified with Pt nanoparticles were tested for comparison. Table 1 shows the list of 8 different electrodes that were characterized and the specifications of their modification.

Carbon cloth cathodes (CC) were made by applying one layer of carbon black nanoparticles and four PTFE diffusion layers on the air side of the carbon cloth according to Cheng et al. [16]. In some cases, a catalyst layer containing $0.5\,mg\,cm^{-2}$ platinum nanoparticles was applied on the water side of the carbon cloth to improve reaction kinetics (CC-Pt). Carbon nanotube mat (CNTM) that contains more than 90% carbon nanotubes was donated by Nanocomp Technologies Inc. (OH, USA) and was used directly as the MFC cathode. The same amount of Pt catalyst was applied in some of the CNTM cathodes for comparison (CNTM-Pt).

Single-walled carbon nanotubes (SWNTs) were synthesized by laser vaporization methods [17,18] at the National Renewable Energy Laboratory (NREL) (CO, USA). The as-prepared nanotubes were purified using a method introduced by Dillon, which consisted of treatment in 3 M nitric acid flux for 16 h, followed by an acetone wash and air burn at $525\,°C$ [17]. Commercially available SWNTs and multi-walled carbon nanotubes (MWNTs) were purchased from CheapTubes Inc. (NJ, USA) and purified by the same procedure. The purified carbon nanotubes were suspended in 1% sodium dodecyl sulfate (SDS) surfactant water solution to prevent agglomeration. The suspended carbon nanotubes were then deposited onto a PTFE membrane (Advantec MFS, Inc., CA, USA) by vacuum filtration to form a compact cathode. Sufficient DI water washing was applied after to remove the extra surfactant. In some cases, Pt nanoparticles ($0.5\,mg\,cm^{-2}$) were uniformly coated on the surface of carbon nanotubes by using a controlled temperature microwave method (250 W, $140\,°C$) for 90 s [19]. The cathodes containing nanotubes synthesized at NREL with and without Pt coatings were labeled as $SWNT_n$-Pt and $SWNT_n$, respectively. Similarly, the cathodes using commercial SWNTs and MWNTs from CheapTubes Inc. with Pt coating were labeled as $SWNT_c$-Pt $MWNT_c$-Pt, respectively (Table 1).

2.2. MFC construction and operation

Single chamber cubic-shaped reactors were constructed as previously described [6,20]. The total volume of each reactor was 28 mL. Graphite fiber brushes were used as the anodes in all of the experiments. Prior to the tests, the brushes were treated by soaking in acetone overnight and then heated at $450\,°C$ for 30 min [21]. All reactors were initially equipped with CC-Pt cathodes and inoculated using effluent from an air-cathode MFC operated for nearly one year. When exoelectrogenic bacteria acclimated and all reactors showed repeatable and comparable voltages ($510 \pm 10\,mV$), nanotube modified air-cathodes were transferred to MFC reactors for performance characterization. Medium solution was prepared containing $1.25\,g\,L^{-1}$ CH_3COONa, $0.31\,g\,L^{-1}$ NH_4Cl, $0.13\,g\,L^{-1}$ KCl, $3.321\,g\,L^{-1}$ $NaH_2PO_4 \cdot 2H_2O$, $10.317\,g\,L^{-1}$ $Na_2HPO_4 \cdot 12H_2O$, $12.5\,mL\,L^{-1}$ mineral solution, and $5\,mL\,L^{-1}$ vitamin [22]. Reactors were operated in fed-batch mode at room temperature and refilled with new medium solution when voltages reduced below 30 mV forming one cycle of operation.

2.3. Electrochemical and microscopy analysis

Voltage across an external resistor ($1000\,\Omega$) was recorded at 10-min intervals using a data acquisition system (Keithley Instrument, OH, USA) connected to a computer. Polarization power density curves were obtained by altering external resistances from $50,000\,\Omega$ to $50\,\Omega$ during the stable power production stage of each batch. The calculations of power density were performed according to Ren et al. [23].

Linear sweep voltammetry (LSV) was applied using a potentiostat (PC4/300, Gamry Instruments, NJ, USA) to characterize the abiotic electrochemical oxygen reduction behavior on different cathodes. LSV tests were conducted in the same reactor filled with same media solution but without carbon source and bacterial inoculum [24]. The working electrode was the cathode ($4.9\,cm^2$ projection area), the counter electrode was a titanium wire (diameter: 0.081 cm, length: 40 cm), and the reference electrode was an Ag/AgCl electrode (RE-5B, BASi, IN, USA). The potential was scanned from open circuit potential to $-0.2\,V$ at a rate of $1.0\,mV\,s^{-1}$. Reactor internal resistances were measured by electrochemical impedance spectroscopy (EIS) with the anode as the working electrode, and the cathode as the counter electrode and reference electrode. The scan range was from 10^5 Hz to 0.005 Hz with a small sinusoidal perturbation of $\pm 10\,mV$ [3]. All tests were repeated at least three times to verify consistency.

Selected cathode samples were examined using a dual beam focused ion beam scanning electron microscope (FIB/SEM, NOVA 600i, FEI Company). Samples were fixed overnight at $4\,°C$ by Karnovsky's fixative (Electron Microscopy Sciences, CA, USA), washed three times in phosphate buffer (0.2 M, pH 7.2), and then dehydrated stepwise in a series of water/ethanol solutions with increasing ethanol concentration (50, 70, 80, 90, 100%). Samples were then kept in a desiccator prior to Pd/Pt sputtering and SEM observation.

3. Results and discussion

3.1. Electrochemical performance

The electrochemical performance of the cathodes with respect to current density was evaluated using LSV tests in the absence of bacteria (Fig. 1). Among the cathodes without Pt catalyst coating, those electrodes consisting of or modified with carbon nanotubes (e.g., CNTM and $SWNT_n$) showed much larger current responses than the carbon cloth cathode (CC). $SWNT_n$ cathodes showed the most positive onset potential, followed by the CNTM cathode, while the CC showed minimal current response across the potential scan range. The larger current response from the nanotube cathodes indicates a higher limiting current density and better electrochemical performance, presumably due to the higher specific surface area

Table 1
List of cathode materials and modifications used in this study and their specifications.

Cathode name	Material type	Pt coating method
CC	Carbon cloth	–
CC-Pt	Carbon cloth with Pt	10%Pt/carbon black mixture (brush)
CNTM	Carbon nanotube mat	–
CNTM-Pt	Carbon nanotube mat with Pt	10%Pt/carbon black mixture (brush)
[a]$SWNT_n$	SWNT coated electrode	–
[a]$SWNT_n$-Pt	SWNT coated electrode with Pt	H_2PtCl_6 (Microwave)
[b]$SWNT_c$-Pt	SWNT coated electrode with Pt	
[b]$MWNT_c$-Pt	MWNT coated electrode with Pt	

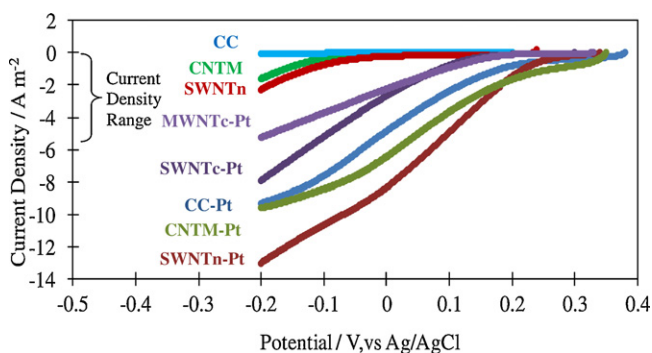[a] Nanotube synthesized in National Renewable Energy Laboratory.
[b] Nanotube purchased from Cheap Tubes Inc.

generated by nanotube modification [25]. In comparison, the flat current response of CC cathodes over the range of voltages examined indicates that the carbon cloth itself did not catalyze oxygen reduction.

The addition of Pt catalyst on the cathodes significantly increased the current densities of all cathodes (Fig. 1). The current densities of CNTM-Pt, $SWNT_n$-Pt, and CC-Pt cathodes all increased substantially compared with their non-Pt counterparts, and the $SWNT_n$-Pt showed the best performance across the potential range. Considering the same amount of catalyst was applied on the electrodes, the LSV results suggest that the 3-D structure created by the carbon nanotubes on $SWNT_n$-Pt allowed more Pt nanoparticles to be deposited inside the electrode space rather than on the surface, leading to increased reaction kinetics [26]. The electrochemical performance of cathodes modified by commercial single-walled nanotubes ($SWNT_c$-Pt) and multi-walled nanotubes ($MWNT_c$-Pt) with Pt coatings were also evaluated using the same LSV tests. In general, both cathodes showed lower current densities compared to the other three electrodes described previously. The reason could be attributed to the different nanotube synthesis approaches. The laser vaporization method used for $SWNT_n$-Pt has been known to produce higher quality nanotubes than the chemical vaporization method used for $SWNT_c$-Pt. The higher crystallization and electric conductivity of $SWNT_n$ resulted in higher electron transfer efficiency thus higher performance. The $SWNT_c$-Pt showed larger current response than the $MWNT_c$-Pt across the scanned potentials. This is presumably due to the high resistance thus more electrochemical loss of MWNTs compared with SWNTs. The resistance of the reactor with the $MWNT_c$-Pt cathode was 94 Ω, which is nearly 3 times higher than with the $SWNT_c$-Pt cathode (35 Ω).
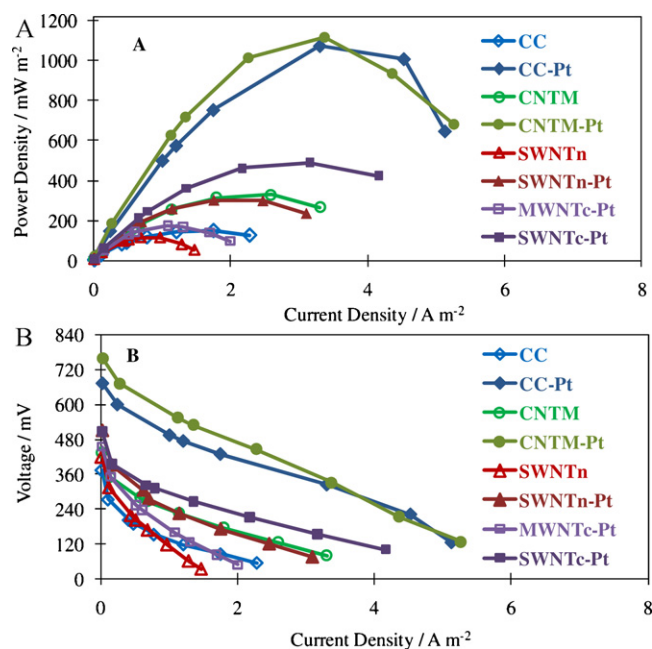
3.2. Performance of MFCs with nano-modified air-cathodes

The nano-modified air-cathodes were transferred to pre-acclimated single chamber MFCs after LSV tests. Rapid voltage

generation was observed in all reactors. Fig. 2 shows the power density and polarization curves obtained from each MFC reactor during steady power production stages. Fig. S1 shows the voltage profiles as a function of time (Supporting information). For MFC cathodes without Pt catalyst coating, CNTM reactor showed the maximum power density of 329 mW m^{-2}, more than twice that of the peak power obtained from CC reactor (151 mW m^{-2}). The $SWNT_n$ reactor showed a lower power density (117 mW m^{-2}) than the other two reactors without Pt. Similar to the results observed during LSV tests, the reactor performance was greatly improved by the application of Pt catalyst in the cathodes. During the first several batches, the power densities of $SWNT_n$-Pt and CNTM-Pt reactors, calculated from voltages at 1000 Ω, were 735 mW m^{-2} and 723 mW m^{-2}, respectively, which were higher than that of CC-Pt reactor (672 mW m^{-2}). The voltages of CNTM-Pt and CC-Pt MFCs kept stable during multiple batches, but the voltage of the $SWNT_n$-Pt reactor decreased gradually from the first batch and stabilized after the fourth batch, resulting in a voltage drop from more than 600 mV to around 300 mV. As shown in Fig. 2, the power density curves obtained at the steady state operation of each reactor show the maximum power densities from CNTM-Pt and CC-Pt MFCs of 1118 mW m^{-2} and 1071 mW m^{-2}, respectively, while the maximum power density of $SWNT_n$-Pt after stabilizing was 302 mW m^{-2}. A similar voltage decline was observed in $SWNT_c$-Pt and $MWNT_c$-Pt MFCs in the first batches. The maximum power

Fig. 1. LSV results (current density vs potential) of newly modified cathodes before installing in MFCs. (Current density range was marked based on the values shown in Fig. 2.)

Fig. 2. Power density as a function of current density (A) and polarization curves (B) for MFCs operated using different air-cathodes.

density produced by $SWNT_c$-Pt was 522 mW m^{-2}, which was about two times higher than that from $MWNT_c$-Pt (174 mW m^{-2}), confirming that SWNT material performs better as MFC cathodes due to its lower ohmic resistance compared with MWNT material.

The electrochemical performance of CC-Pt and $SWNT_n$-Pt cathodes were analyzed again by LSV tests after MFC operation in order to understand the chemical and microbial effects on the cathode performance. Fig. 3 shows the electrochemical performance of the used CC-Pt cathode decreased slightly compared with the new cathode, while the current response of the used $SWNT_n$-Pt cathode declined significantly compared with the new $SWNT_n$-Pt. This drop may explain why the steady state power density of the $SWNT_n$-Pt reactor was lower than the CNTM-Pt and CC-Pt reactors despite a better LSV performance with new $SWNT_n$-Pt cathodes. Such finding could also be confirmed by the changes of open circuit potential (OCP). The OCP of the $SWNT_n$-Pt cathode dropped by 35%, from 357 mV in batch 1 to 233 mV in batch 4, while the OCP of CC-
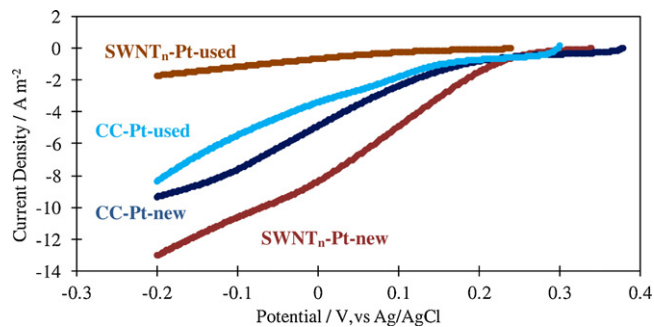

Fig. 3. Comparison of LSV electrochemical test results between new and used cathodes of CC-Pt and $SWNT_n$-Pt.
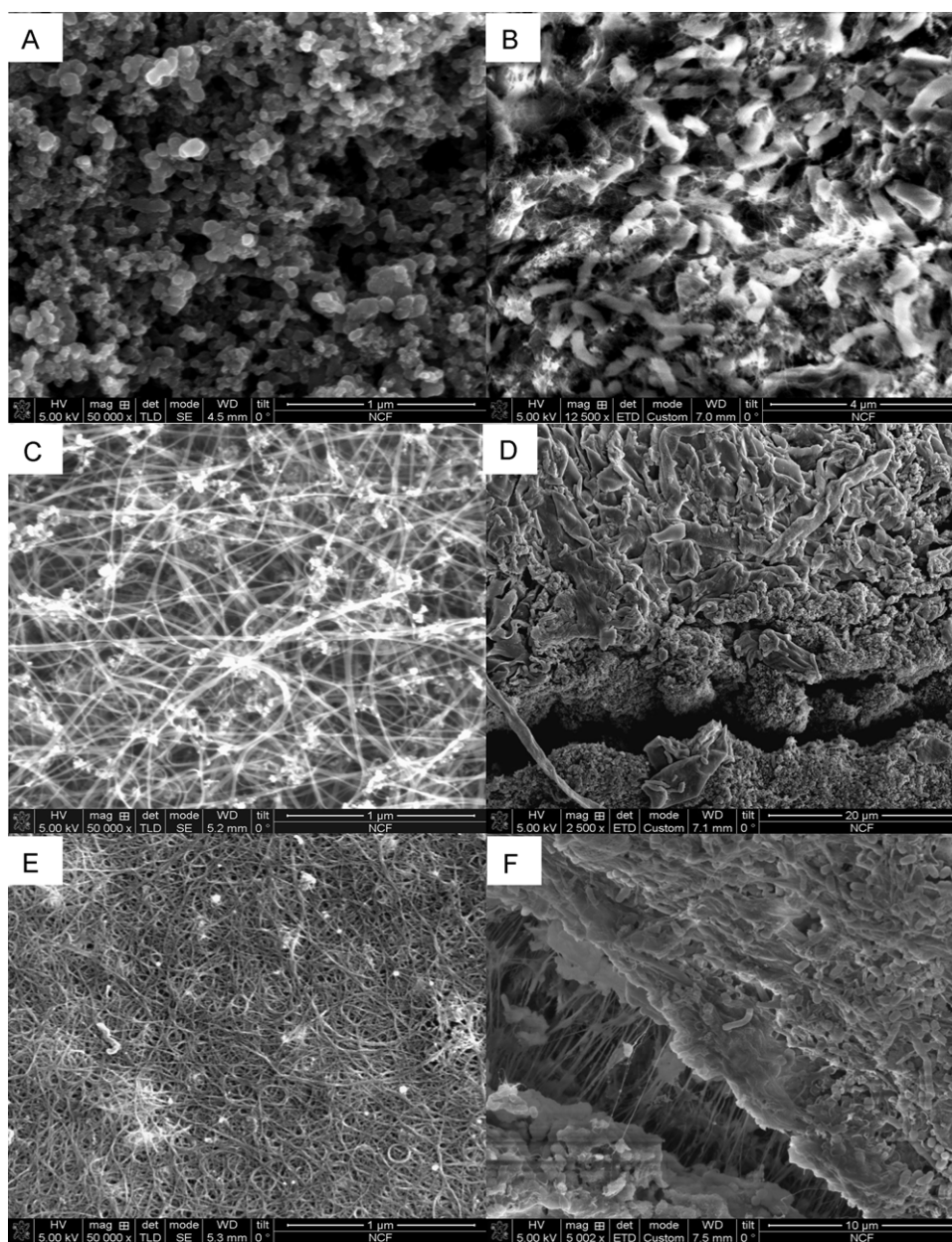

Fig. 4. SEM/FIB images of new and used cathodes: (A) new CC-Pt, (B) used CC-Pt after MFC operation, (C) new CNTM, (D) used CNTM-Pt after MFC operation, (E) new $SWNT_n$-Pt, and (F) used $SWNT_n$-Pt after MFC operation.

Pt only dropped by 9%, from 345 mV to 310 mV during the same period. Similar findings in air-cathode performance decline were reported by several other studies, and the reasons were believed to be due to the adherence of biofilm and chemical deposits on the cathode surfaces that reduced charge transfer and catalyst activity [27,28]. For the SWNT$_n$-Pt cathode, the large amount of pores, cavities, and curving paths among carbon nanotubes that increase the specific surface area also enables adsorption of impurities that may cover the surfaces of the cathode and reduce charge transfer. Adding a separator on the nanotube modified electrode to block adsorption or switching the nanotube layer to the air-face side could be possible solutions [29,30]. It may also be possible that the SWNTn-Pt cathode performance decreased due to the loss of the Pt catalyst overtime since the microwave deposition method has not been optimized for MFC operation. However, this was not confirmed using energy dispersive spectroscopy element percentage test during FIB/SEM characterization.

3.3. FIB/SEM analysis

Scanning electron micrographs were taken for the CC-Pt, CNTM-Pt, and SWNT$_n$-Pt cathode materials before and after MFC operation. Fig. 4 shows a distinct difference in morphology between the new CC-Pt cathode and new CNTM-Pt and SWNT$_n$-Pt cathodes. The CC-Pt cathode surface was covered by aggregated particles or short fibers (Fig. 4A), while the new CNTM- Pt and SWNT$_n$-Pt electrode surfaces clearly showed the carbon nanotube network (Fig. 4C and E). The deposited Pt catalyst shows up in the images as bright nanoparticles deposited across the nanotube network.

Denser microbial biofilms were formed on the surface of the CC-Pt cathode (Fig. 4B) compared with the CNTM-Pt and SWNT$_n$-Pt cathodes (Fig. 4D and F), but more chemical deposit covered a large portion of the surface of the two CNT-modified electrodes. Studies showed that the excess accumulation of biofilm and chemical scales [27,28] could adversely affect the system performance due to the decrease in active cathode specific surface area and increase in diffusion resistance in oxygen. Such observations may also explain the reduced electrochemical activities in certain MFCs after a period of operation, where the presence of cavities and the adsorption of impurities played a major role as compared to cathode biofilms.

4. Conclusions

Microbial fuel cells provide direct and efficient electricity generation from renewable sources, but the current 2-D air-cathode configuration limits system performance due to the low kinetics of oxygen reduction. Carbon nanotubes were used in this study to modify air-cathodes in single chamber MFCs to create a 3-D structure for improved surface area and reaction kinetics. Compared with traditional carbon cloth cathodes, all nanotube modified cathodes showed greater electrochemical performance as well as higher power density in MFCs. The maximum power density obtained from carbon nanotube mat cathodes (329 mW m^{-2}) was more than double the power output from traditional carbon cloth cathodes (151 mW m^{-2}). The addition of Pt catalyst on the cathodes increased the current densities of all cathodes, with the maximum power density achieved by a CNTM-Pt of 1118 mW m^{-2}. Electrodes made from commercial single wall carbon nanotubes (SWNT$_c$-Pt) have much lower ohmic resistance than those made from multi-wall nanotubes (MWNT$_c$-Pt) and showed larger current response and higher power. The customized SWNT$_n$ electrode showed great

electrochemical responses, but its performance declined gradually due to the deposition of chemical and microbial impurities which blocked reaction surfaces. Scanning electron micrographs demonstrated different electrode surface morphologies, with the CNT modified cathodes showing carbon nanotube networks and carbon cloth cathodes showing aggregated particles on the electrode surface.

Acknowledgements

Appendix A. Supplementary data

Supplementary data associated with this article can be found, in the online version, at doi:10.1016/j.jpowsour.2011.05.005.

References

[1] B.E. Logan, Microbial Fuel Cells, John Wiley & Sons, New York, 2008.
[2] K. Rabaey, P. Clauwaert, P. Aelterman, W. Verstraete, Environ. Sci. Technol. 39 (2005) 8077–8082.
[3] Z. Ren, R.P. Ramasamy, S.R. Cloud-Owen, H. Yan, M.M. Mench, J.M. Regan, Bioresour. Technol. 102 (2011) 416–421.
[4] S. Cheng, B.E. Logan, Electrochem. Commun. 9 (2007) 492–496.
[5] Z. He, N. Wagner, S.D. Minteer, L.T. Angenent, Environ. Sci. Technol. 40 (2006) 5212–5217.
[6] B. Logan, S. Cheng, V. Watson, G. Estadt, Environ. Sci. Technol. 41 (2007) 3341–3346.
[7] Y.Z. Fan, E. Sharbrough, H. Liu, Environ. Sci. Technol. 42 (2008) 8101–8107.
[8] H. Rismani-Yazdi, S.M. Carver, A.D. Christy, I.H. Tuovinen, J. Power Sources 180 (2008) 683–694.
[9] F. Zhao, F. Harnisch, U. Schroder, F. Scholz, P. Bogdanoff, I. Herrmann, Environ. Sci. Technol. 40 (2006) 5193–5199.
[10] Q. Deng, X. Li, J. Zuo, A. Ling, B.E. Logan, J. Power Sources 195 (2010) 1130–1135.
[11] S. Cheng, B.E. Logan, Bioresour. Technol. 102 (2011) 4468–4473.
[12] P. Liang, H. Wang, X. Xia, X. Huang, Y. Mo, X. Cao, M. Fan, Biosens. Bioelectron. 26 (2011) 3000–3004.
[13] X. Xie, L. Hu, M. Pasta, G.F. Wells, D. Kong, C.S. Criddle, Y. Cui, Nano Lett. 11 (2011) 291–296.
[14] J.L. Lamp, J.S. Guest, S. Naha, K.A. Radavish, N.G. Love, M.W. Ellis, I.K. Puri, J. Power Sources 196 (2011) 5829–5834.
[15] H.-Y. Tsai, C.-C. Wu, C.-Y. Lee, E.P. Shih, J. Power Sources 194 (2009) 199–205.
[16] S. Cheng, H. Liu, B.E. Logan, Electrochem. Commun. 8 (2006) 489–494.
[17] A.C. Dillon, T. Gennett, K.M. Jones, E.L. Alleman, P.A. Parilla, M.J. Heben, Adv. Mater. 11 (1999) 1354–1358.
[18] A. Thess, R. Lee, P. Nikolaev, H. Dai, P. Petit, J. Robert, C. Xu, Y.H. Lee, S.G. Kim, A.G. Rinzler, D.T. Colbert, G.E. Scuseria, D. Tomanek, J.E. Fischer, R.E. Smalley, Science 273 (1996) 483–487.
[19] C.-M. Chen, M. Chen, H.-W. Yu, S.-C. Lu, C.-F. Chen, Jpn. J. Appl. Phys. 47 (2008) 2324–2329.
[20] H. Liu, B.E. Logan, Environ. Sci. Technol. 38 (2004) 4040–4046.
[21] X. Wang, S. Cheng, Y. Feng, M.D. Merrill, T. Saito, B.E. Logan, Environ. Sci. Technol. 43 (2009) 6870–6874.
[22] H. Luo, P.E. Jenkins, Z. Ren, Environ. Sci. Technol. 45 (2011) 340–344.
[23] Z. Ren, H. Yan, W. Wang, M. Mench, J. Regan, Environ. Sci. Technol. 45 (2011) 2435–2441.
[24] F. Zhang, T. Saito, S. Cheng, M.A. Hickner, B.E. Logan, Environ. Sci. Technol. 44 (2010) 1490–1495.
[25] J.R. Kim, J.-Y. Kim, S.-B. Han, K.-W. Park, G.D. Saratale, S.-E. Oh, Bioresour. Technol. 102 (2011) 342–347.
[26] S. Cheng, P. Kiely, B.E. Logan, Bioresour. Technol. 102 (2011) 367–371.
[27] P.D. Kiely, G. Rader, J.M. Regan, B.E. Logan, Bioresour. Technol. 102 (2011) 361–366.
[28] K. Chung, I. Fujiki, S. Okabe, Bioresour. Technol. 102 (2011) 355–360.
[29] O. Lefebvre, W.K. Ooi, Z. Tang, M. Abdullah-Al-Mamun, D.H. Chua, H.Y. Ng, Bioresour. Technol. 100 (2009) 4907–4910.
[30] S. Yang, B. Jia, H. Liu, Bioresour. Technol. 100 (2009) 1197–1202.